

Fabrication of high strength and a low weight composite bipolar plate for fuel cell applications

Priyanka H. Maheshwari*, R.B. Mathur, T.L. Dhami

Carbon Technology Unit, Division of Engineering Materials, National Physical Laboratory, New Delhi 110012, India

Received 7 February 2007; received in revised form 13 April 2007; accepted 13 April 2007

Available online 4 May 2007

Abstract

The bipolar plate is one of the most important components in a PEM fuel cell. A polymer composite bipolar plate possessing high strength (81 MPa) and high stiffness (20 GPa) has been developed by making use of carbon fiber network in a specific form as the filler component. Such high strength is very much desired, especially when the fuel cells are used for mobile applications, since it is the bipolar plate that provides mechanical support to all the other cell components. The addition of carbon black and the effect of particle size of the natural graphite flakes used as other reinforcements also play a crucial role in controlling the physical and electrical properties of the composite plates. The plate when used in the unit fuel cell assembly showed I – V performance comparable to that of the commercially available bipolar plates.

© 2007 Elsevier B.V. All rights reserved.

Keywords: Fuel cell; Electrode; Electrical resistivity; Porosity

1. Introduction

Polymer electrolyte membrane fuel cells are the potentially most promising and clean power sources for road transportation and portable applications [1]. The key components of a fuel cell are the electrolyte, catalyst layer, gas diffusion layer and bipolar plate [2]. The bipolar plate which accounts for 80% by weight and 60% by cost of the fuel cell stack has several functions: (i) to separate the individual fuel cells from each other, (ii) to electrically connect them in series, (iii) to provide a gas “flow field” (channels are etched into the side of the plate next to the backing layer to carry the reactant gases from the place where it enters the fuel cell to the place where it exits), (iv) to provide a physical barrier to avoid mixing of the oxidant, fuel and coolant fluids, (v) to provide mechanical support to the other cell components, (vi) to conduct heat and electricity between cells and (vii) to allow the cooling of the cells. Hence, the bipolar plate must be inexpensive, easy to machine or shape and lightweight. It should also possess good electrical conductivity, high strength, thermal stability and corrosion resistance [3,4].

The most commonly used bipolar plate material is graphite. Although it is resistant to corrosion and has low bulk resistivity, the brittleness of graphite requires a thickness of the order of several millimeters (8–10 mm) causing the fuel cell stack to be heavy and voluminous [5].

Metal is also a good material for bipolar plate. It offers good electrical conductivity, excellent mechanical properties and ease of fabrication, but is unable to resist corrosion in fuel cells. Corrosion of the metal bipolar plate leads to a release of multivalent cat ions, which can lead to an increase in membrane resistance and to the poisoning of the electrode catalyst [6–9]. Titanium offers excellent electrical performance and power densities, but it is expensive and requires precious metal coatings for durability. Stainless steel however offers reasonable power and low material and production costs but gives lower gravimetric performance and may require application of a coating to make it resistant to corrosion.

Composite bipolar plates are an attractive option for PEM fuel cell use. They not only offer the advantage of low cost, lower weight and greater ease of manufacture than traditional graphite but also their properties can be tailored by changing different reinforcements and the resin systems. Two different types of resins are used to fabricate composite plates: thermoplastic and thermosetting.

* Corresponding author. Tel.: +91 11 25746290; fax: +91 11 25726938.
E-mail address: hedap@mail.nplindia.ernet.in (P.H. Maheshwari).

Thermoplastic composite materials for use in fuel cell bipolar plates are described in U.S. Pat. No. 4,214,969 (Lawrence) and U.S. Pat. No. 4,339,322 (Balco et al.). The '969 patent describes a molded graphite/poly (vinylidene fluoride) material [10], and the '322 patent claims improvements in the mechanical properties of the same with the addition of carbon fibers [11]. Thermoplastic resins form dry mixtures suitable for compression molding when combined with graphite powder. However, the composite must be allowed to cool before removal from the mold, by cold water flowing through the platens of the hydraulic press. Thermosetting resins (e.g., phenolics, epoxies and vinyl esters) can be removed from the mold without cooling, offering shorter process times.

Carbon/carbon composite plates developed at Oak Ridge National Laboratory [12] use slurry molding of chopped carbon fiber with phenolic resin, followed by sealing with chemically vapor-infiltrated carbon (CVI). Although the above process imparts high electronic conductivity and flexural strength, it is not cost effective.

Exfoliated graphite is available readily and is inexpensive. It is electrically conducting, corrosion resistant, and is self-sealing, which obviates the requirement for separate gaskets. A bipolar plate can be built up from a number of cut foils [13]; or can be prepared by embossing flow fields on sheets of compressible, electrically conductive material, i.e. a graphite foil [14]. Very high performance is obtained with this material since it is compressible and thus interfacial resistance is minimized within the cell. However this compressibility complicates the construction of fuel cell stack, as it is difficult to maintain uniform flow fields and gas access to each cell.

Emanuelson et al. developed a thinner flat plate with a phenolic resin content of 50% and a thickness of 0.75 mm [15]. These plates however operated successfully for 2 years in the PC-18 40 kW power plant.

Showa Denko developed the process for manufacturing a separator plate that laminates several piles of a felt that contains cellulose fibers, graphite powder and phenolic resin to form a mold blank, which is then carbonized, and graphitized [16], making the entire process costly.

The present study aims at developing a conducting polymer composite plate for fuel cell applications incorporating the advantage of high mechanical strength, much higher than that of the existing commercially available plates. High strength will allow thinner plates to be fabricated thus reducing the overall weight of the fuel cell stack. The plates of thickness 2.4 mm developed by us were found to take greater load before fracture as compared to the conventional graphite plates with thickness of 7–8 mm and the commercially available composite plates (Grade FU 4369) from M/s Schunk GmbH with thickness 4 mm. This will greatly reduce the cost and weight of the fuel cell stack.

Since the bipolar plate needs to be highly conductive, natural graphite (NG) constituted a major fraction (65 vol.%) of the plate component. Thermosetting phenolic resin (25 vol.%) has been used as a binder, which not only creates very low open porosity but is also cost effective. The remaining 10% of the reinforcement constituted different ratios of carbon fiber (CF) and carbon black (CB). Use of carbon fibers in a special form has been tried,

unlike the conventional trend of using them in the chopped form and in random orientation [17]. The composite plates developed in the present study possess flexural strength as high as 81 MPa and the compressive strength value of 84 MPa. Such high values have not been reported so far [4,12,14,17–19]. In the experimental series so performed we choose to study the comparative effect of carbon fiber mat and carbon black on the various properties of the bipolar plate, while keeping the amount of natural graphite (65 vol.%) and the binder resin (25 vol.%) constant. Studies were also carried out using different sizes of graphite particles (NG), as it greatly affects the process ability and hence the various physical and electrical properties of the composite plate. In such experiments the amount of fiber and carbon black was kept constant at 2.5 and 7.5 vol.%, respectively.

2. Experimental

The composite plate was prepared in following two steps:

2.1. Preparation of the carbon fiber preform

The first step involves the preparation of a thin, porous carbon fiber skeleton or mat by paper making technology. Unidirectional tows of commercial grade 6K T-300 Toray carbon fibers (T.S. = 3.5 GPa; Y.M. = 230 GPa) were chopped to lengths of 10 mm for making the fiber preform [20]. A number of performs of size 10 cm × 10 cm were thus prepared. The optical micrograph of the carbon fiber preform is shown in Fig. 1. The preform has density 0.1 g cm^{-3} and porosity between 75% and 85%.

2.2. Preparation of the composite bipolar plate

In the second step several perform layers were sandwiched between the thick slurry comprising of filler carbons and the resin. Phenolic resin obtained from 'IVP India Ltd.' was used as a carbonaceous resin for making the composite plate because of its high carbon yield and low cost. Natural graphite lumps

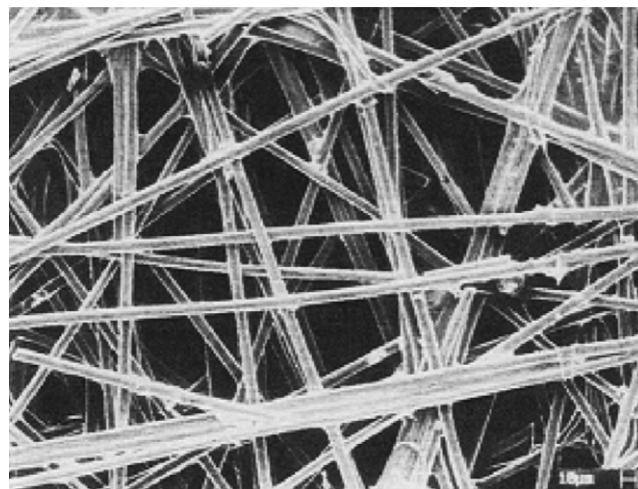
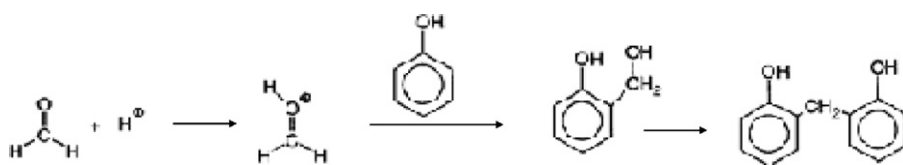


Fig. 1. SEM of a carbon fiber preform.

of density 2.2 g cm^{-3} were pulverized and then ball milled to several hours. The powder was sieved to obtain different particle size fractions, viz. 149–99, 99–74, 74–49, 49–37 μm and less than 37 μm , respectively, and used as filler materials. Small fraction of carbon black obtained by thermal decomposition of hydrocarbons was also used as one of the filler components.

Calculated amounts of NG powder and CB were mixed together and added to the phenolic resin dissolved in acetone as solvent. The mix was stirred thoroughly to obtain thick slurry by evaporating the solvent. The slurry was uniformly applied on the calculated number of porous carbon fiber performs. The impregnated sheets were dried, stacked together and put in a die mould that was then placed between the platens of the hydraulic press. A pressure of 50 kg cm^{-2} was applied when the temperature reached 90°C . The temperature was then gradually raised and the final curing temperature of the resin was maintained at 150°C for 1 h. The polymerization of the resin occurs by electrophilic aromatic substitution between the ortho and para positions of phenol and protonated formaldehyde as shown below. Methylene bridges between phenol molecules make the final cross-linked polymer.



2.3. Characterization of the molded plates

The physical and electrical properties of the composite plates were evaluated before the single cell test. The in plane and the bulk electronic conductivities were measured by four-probe technique. Kiethley 224 programmable current source was used for providing current. The voltage drop along the various points of the plate was measured by Kiethley 197 A auto ranging micro volt DMM. An average of ten readings is reported in the text.

Gas permeability of the plate was determined using the apparatus as shown in Fig. 2. The sample is placed in between two hollow metal discs (comprising the sample holder) and sealed with the help of metal screws and rubber *o*-rings. One face of the sample holder is connected to gas cylinder via a pressure gauge, while water is poured on the other face of the sample. The line pressure (p) of the gas is increased gradually till the bubbling in water above the sample surface is noted. The sample is thus treated as impermeable up to the pressure $\leq p$.

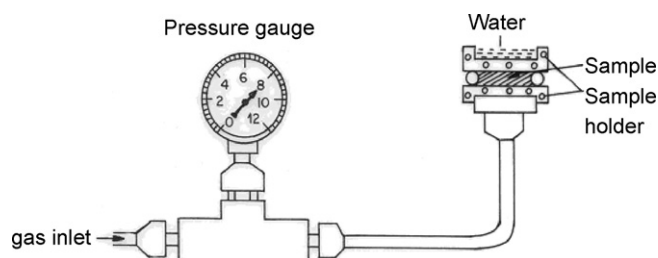


Fig. 2. Experimental set-up to determine the gas permeability.

Surface hardness of the bipolar plate samples was measured by means of a Scleroscope, hardness tester obtained from 'Coats Machine Tool Co. Ltd. London'. A metal ball is allowed to strike the surface of the sample and correspondingly the hardness is read on the vertical scale to which the ball bounces back.

The surface energy of the bipolar plate samples was measured by dynamic contact angle (θ) measurements using Wilhelmy method on a 'CAHN Dynamic Contact Angle Analyzer, DCA-322'.

The porosity, density and water adsorption of the samples were determined according to the ASTM C 20, D 792 and D 570 test procedures, respectively. The mechanical properties of the composite plates were measured on the INSTRON machine model-4411. The flexural and the compressive strength were measured using ASTM D 1184-69 and D 3410-75 test procedures, respectively. The microstructure of the composite bipolar plate was examined under polarized light by means of a Zeiss model optical microscope MC 80 DX and the fractured surfaces of the samples were observed under the SEM, model Leo S-440.

2.4. Single cell test

The composite plates were used in pair for their I - V performance on a single cell assembly prepared as discussed below.

The electrodes of the cell were prepared by coating carbon (Vulcan XC-500 obtained from Cabot Corporation, USA) and PTFE on the wet-proofed Toray carbon paper. The carbon and PTFE loadings were maintained at a fixed content of 1.5 and 0.225 mg cm^{-2} , respectively. To prepare the catalyst layer the catalyst, Nafion and isopropyl alcohol were mixed and brushed on to the diffusion layer. The catalyst (Pt, supported on 45 wt% carbon) and Nafion loadings were kept at 0.5 and 0.065 mg cm^{-2} respectively. The anode and the cathode were prepared with the same amount of loadings. The MEA was fabricated by placing the electrodes at both sides of Nafion membrane – 1135 (89 μm) followed by hot pressing at 130°C and 38 kN for 90 s.

Flow field channels were etched on the bipolar plate surface in parallel design. The channel (flow field) and shoulder (current collector) width were kept at 1 and 0.5 mm, respectively, while the channel depth was kept at 0.75 mm.

A single cell was constructed from the prepared MEA, Teflon gaskets and the as prepared composite bipolar plate on both sides of the MEA. Copper sheets were placed on either side to provide external electrical circuit connections and the whole cell was compressed between aluminum end plates, held together with tie-rods.

The hydrogen and the oxygen gases were fed to the anode and cathode, respectively. The fuel cell was operated at 60°C and 100% humidified conditions. The gas stoichiometry for both the

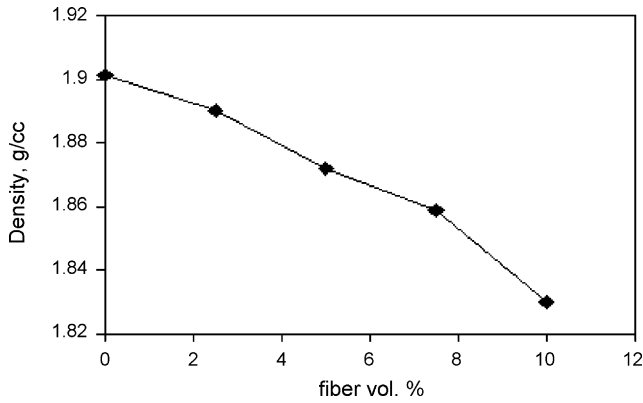


Fig. 3. Variation in the density of the composite plate with increasing fiber content.

gases was kept at 1.5 slpm. The fuel cell was also operated using air instead of oxygen as an oxidizing agent, while maintaining identical operating conditions as discussed.

3. Results and discussion

3.1. Density

Fig. 3 shows the variation in the density of the plate with different fiber volume fractions. The density of the plate decreases from 1.9 to 1.83 g cm⁻³ with increasing fiber content from 0% to 10%. Since the low density component i.e. carbon fiber (density 1.76 g cm⁻³) is added at the cost of carbon black (density 2 g cm⁻³), the density of the composite bipolar plate decreases with increasing fiber content.

Fig. 4 a shows the effect of the particle size on the density of the plate. The density of the composite bipolar plate decreases with decrease in the particle size of NG from 1.92 (149–99 μm) to 1.84 g cm⁻³ (<37 μm). Decreasing particle size would increase the total number of particles and correspondingly the total surface area or the volume of filler interface thereby necessitating higher volume fraction of the resin to wet the complete available surface of NG. As a result the required degree of compaction could not be achieved in the plate, even though the material weight and the applied pressure remained the same. This causes an increase in the thickness

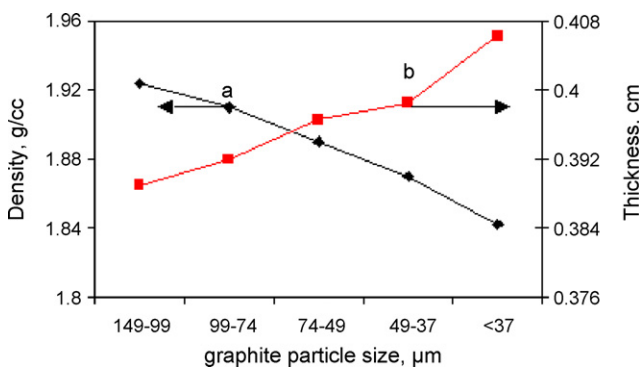


Fig. 4. Variation in the (a) density and (b) thickness of the composite plate with decreasing graphite particle size.

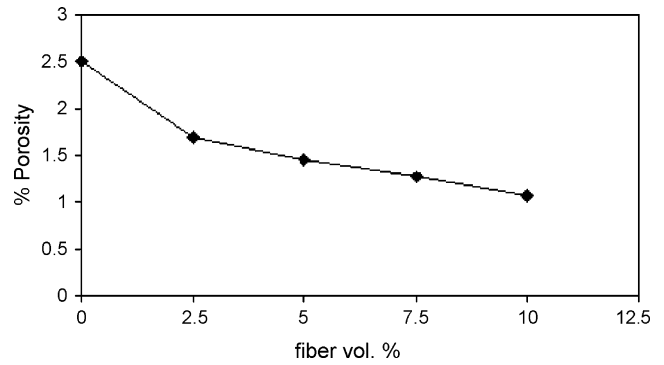


Fig. 5. Variation in the porosity of the composite plate with increasing fiber content.

(Fig. 4b) and corresponding decrease in the density of the plate.

3.2. Porosity and gas permeability

The porosity of the composite bipolar plate decreases gradually with increasing fiber content and reaches a minimum of 1.08% for 10% fiber content (Fig. 5). The porosity arises due to the cross-linking reaction in the resin during the hot pressing process. Both T-300 based carbon fiber and carbon black has almost similar surface energy (greater than that of graphite) and correspondingly the wetting efficiency with the resin. Carbon black however possesses greater surface area as compared to carbon fiber and therefore requires more amount of resin for proper bulk compaction. The porosity of the samples therefore increases with decreasing amount of fiber and increasing amount of carbon black.

The particle size of the graphite also plays an important role in controlling the porosity of the composite. The porosity of the composite plate increases with decreasing particle size from 1.1% (149–99 μm) to 2.82% (for graphite particle size <37 μm) as shown in Fig. 6. Generally it is expected that the finer graphite particles should result in a greater compaction of the composite, leading to very small sized pores. However decreasing particle size increases the overall surface area. Thus the particles are not completely wetted by the resin as explained in Section 3.1. This causes a reduction in the bulk compaction of the material

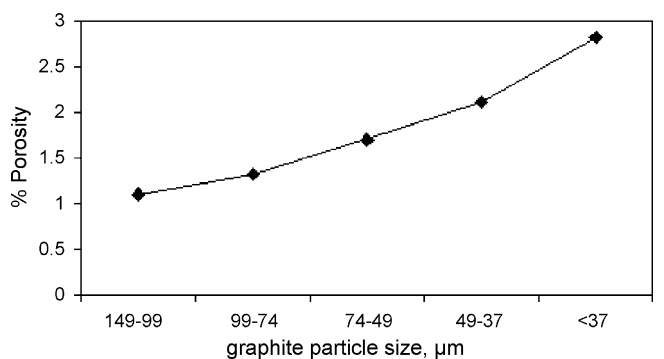


Fig. 6. Variation in the porosity of the composite plate with decreasing graphite particle size.

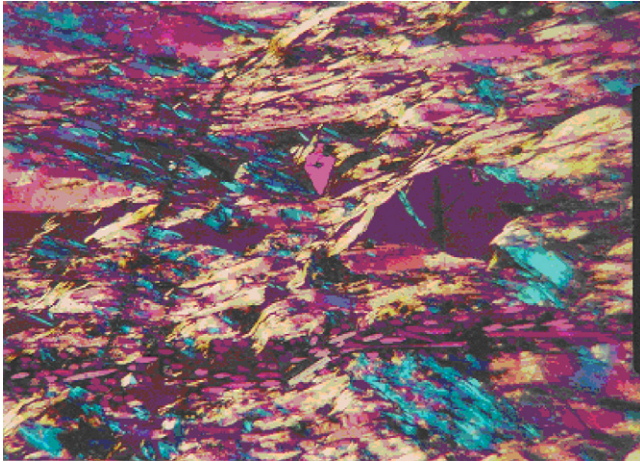


Fig. 7. Optical micrograph of the sample with graphite particle size in the range 149–99 μm (20 \times).

resulting in the formation of voids. This is clear from the optical micrographs of the samples prepared with different graphite particle sizes (Figs. 7 and 8).

The gas permeability test performed on all the samples show that the plates remain impermeable to oxygen gas even at a pressure of 6 kg cm^{-2} . The reason could be the strong bonding of the matrix with the carbon fiber scaffolding and the advantage with the phenolic resin that develops closed porosity during the curing cycle.

3.3. Electrical properties

The in plane electrical resistivity of the composite plate increases with increasing volume fraction of fiber from 0.0033 Ωcm (2.5% CF, 7.5% CB) to 0.0046 Ωcm (10% CF, no CB) as shown in Fig. 9a. Although the major conductive component is graphite, the addition of carbon black further helps in filling the micro pores in the composites, thus facilitating percolation of current [21]. The through plane electrical resistivity of the plate also shows the similar behavior with increasing volume fraction of carbon fibers as shown in Fig. 9b. In both the cases it becomes quite clear that carbon black plays a major role in

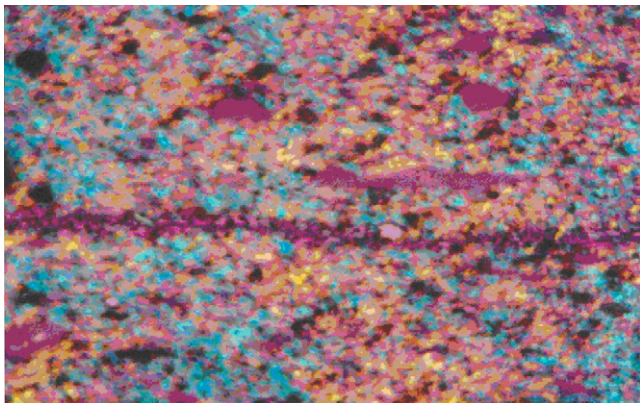


Fig. 8. Optical micrograph of the sample with graphite particle size in the range <37 μm (10 \times).

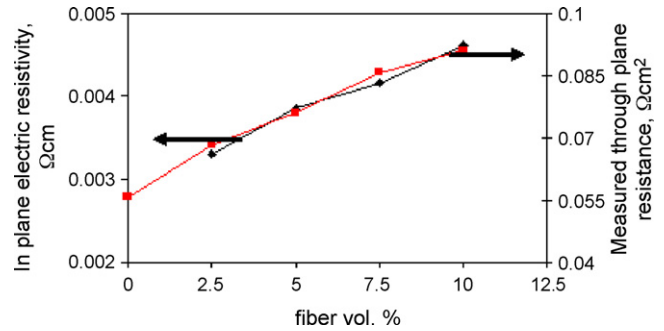


Fig. 9. Variation in the (a) in plane electrical resistivity and (b) measured through plane resistance of the composite plate with increasing fiber content.

improving the electrical conductivity of the composite plate by providing percolation sites [21].

The in plane electrical resistivity of the composite plate increases from 0.00323 Ωcm to 0.00468 Ωcm as the particle size of graphite decreases from 149–99 to <37 μm as shown in Fig. 10a. Decreasing the particle size leads to an increase in the number of particles, this increases the contact resistance and consequently the overall in plane resistivity of the samples.

However the through plane electrical resistivity of the plate was found to decrease with particle size as shown in Fig. 10b. Larger graphite particles tend to align themselves along the plane of the plate during lateral material flow in the molding process. It is for this reason that the through-plane resistivity of the composite is larger by an order of magnitude than the in plane electrical resistivity. The electrical resistivity of single graphite flake is an order of magnitude higher across the basal plane as compared to the in plane value [22]. By decreasing the particle size the orientation effect of the NG particles in the composite plate decreases and almost vanishes for particle size <37 μm (Figs. 7 and 8). The particle at this stage almost becomes spherical in shape as shown in the optical micrograph in Fig. 8. However, the through plane resistivity values plotted in Figs. 9b and 10b does not give the true value of the resistivity of the plate, since it includes twice the contact resistance between the composite plate and the copper plates used as contacts.

More important in the case of a fuel cell is the interfacial contact resistance between the bipolar plate and the carbon paper. To measure the contact resistance, an experimental set-up was devised as shown in Fig. 11. A composite plate was placed in

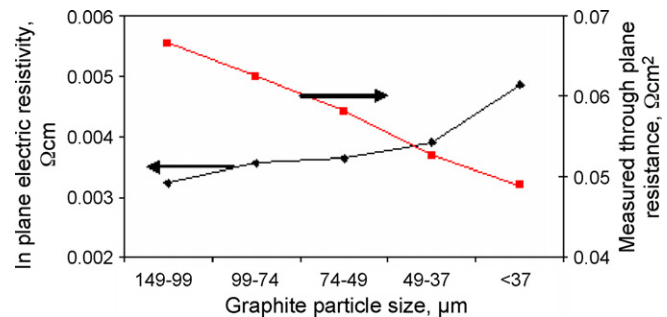


Fig. 10. Variation in the (a) in plane electrical resistivity and (b) measured through plane resistance of the composite plate with decreasing graphite particle size.

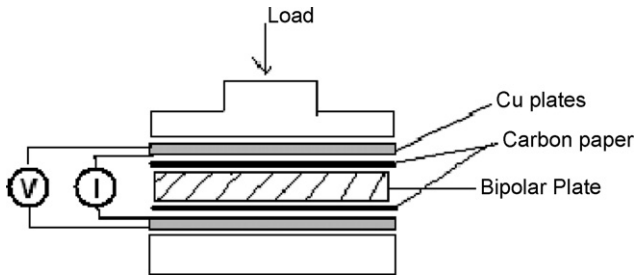


Fig. 11. Experimental set-up to measure the contact resistance.

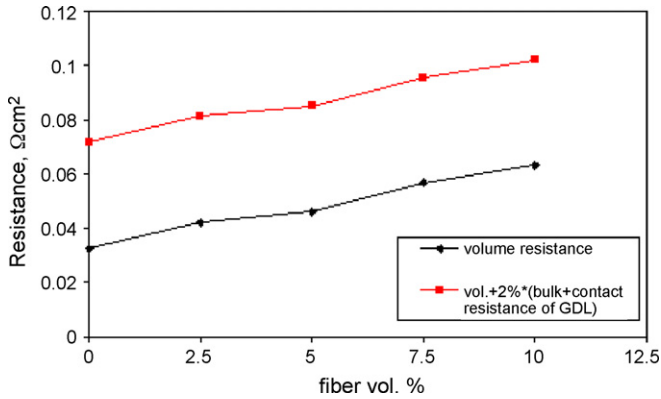


Fig. 12. Variation in the resistivity of the composite plate with increasing fiber content.

between two Toray carbon papers each of which was in contact with a copper plate. While a constant current was passed through the copper plates, the potential difference between the copper plates was measured. The same experiment was then repeated by placing only the carbon paper between the copper plates. The variation in the volume resistance (bulk resistance of the bipolar plate + 2* (interfacial contact resistance between the composite bipolar plate and the Toray carbon paper)) and the total resistance of the set up (volume resistance + 2* (bulk & contact resistance of the carbon paper)) is shown in Figs. 12 and 13. The measurements were taken at a compaction pressure of 4 kg cm⁻².

The volume resistance of pure graphite plate was found to be 0.035 Ωcm². An interesting fact here reveals that although the values of in plane (0.001 Ωcm) and through plane (0.005 Ωcm) resistivities of pure graphite plate are very less [22] as compared to the composite plate values, the volume resistance is almost

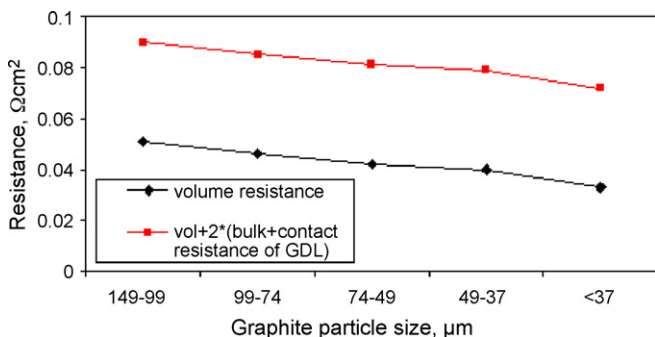


Fig. 13. Variation in the resistivity of the composite plate with decreasing graphite particle size.

of the same order. The result can be attributed to the fact that by compressing the carbon composite, carbon powders formed a compact network. Thus, the ohmic resistance of a fuel cell is expected to be more or less similar while using either the graphite or the composite bipolar plates.

3.4. Mechanical properties

The flexural strength and the flexural modulus of the composite plates developed with different volume percent of carbon fibers is plotted in Fig. 14. As observed the strength as well as modulus registers sharp increase up to 7.5 vol.% of carbon fiber. The strength of the plate increases from 34 to 82 MPa i.e. an overall improvement of 140%. The commercial composite plates (Grade FU 4369) from M/s Schunk GmbH report a value of 40 MPa for the flexural strength of the bipolar plate. The flexural modulus of the plates also shows similar behavior and the value of 20 GPa is achieved with 7.5 vol.% of CF reinforcement. The value is almost double than that of the Schunk plate (FM = 10 MPa). Such strong and stiff plates can prove extremely beneficial for fuel cells used in automobiles where the stack has to withstand sudden impacts and jerks. It is also observed that beyond 7.5 vol.% of CF reinforcement there is hardly any improvement in the mechanical properties. It is suggested that the carbon fiber network introduced in the matrix inhibits the crack propagation and also provides an efficient medium for load transfer. Similarly introducing the stiff phase in the form of fiber network within the sample resists the deformation against applied stress, because of the higher modulus of the carbon fibers.

The SEM micrographs of the fractured surface of the composite plate with 7.5 wt% fibers are shown in Fig. 15a and b. The micrograph in Fig. 15a clearly show fiber pull out as well as broken fibers, suggesting that the fracture is not brittle and the load is effectively transferred to the fibers. Interestingly the rest of the carbon fiber preform inside the sample plate is not disturbed suggesting strong fiber matrix interactions (Fig. 15b). This could be the reason for higher strength and modulus of the plates. The fractured surface of the composite plate without carbon fiber preform (Fig. 16) is quite smooth suggesting a brittle failure of the material.

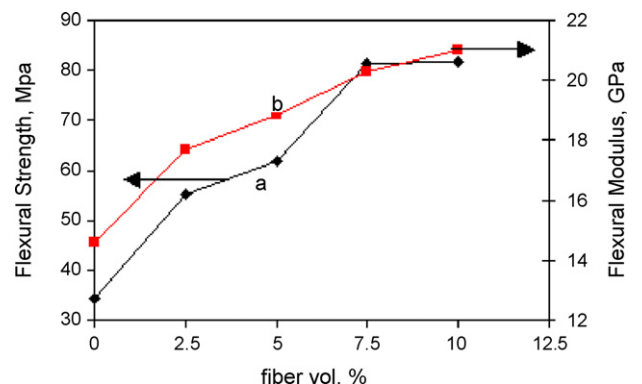


Fig. 14. Variation in the (a) flexural strength and (b) flexural modulus of the composite plate with increasing fiber content.

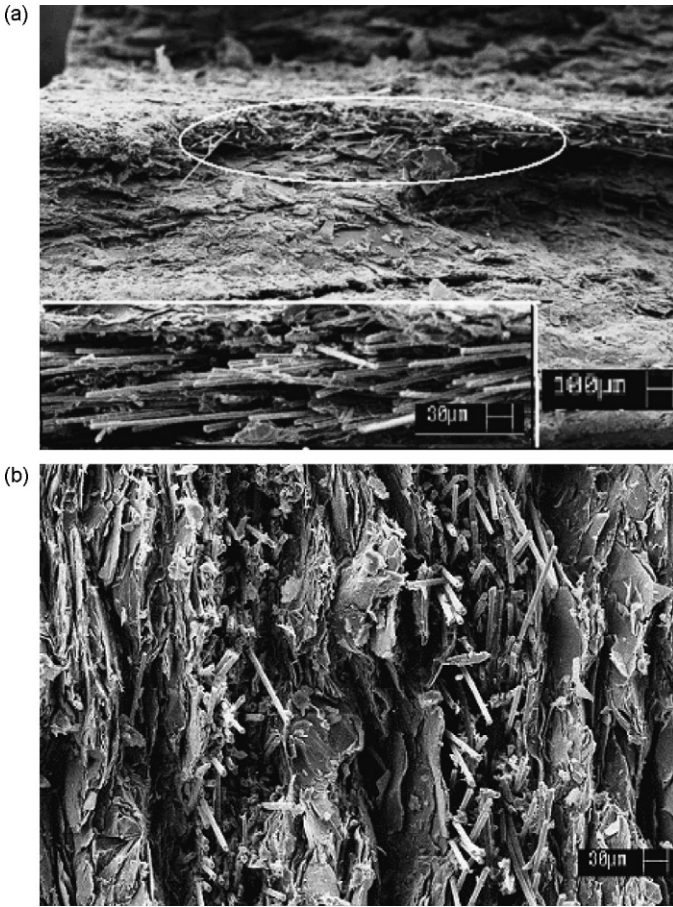


Fig. 15. SEM of the fractured surface of the composite plate with 7.5 vol.% fibers.

The variation in the flexural strength of the carbon paper with decreasing graphite particle size is shown in Fig. 17a. Initially the strength of the composite increases with decreasing particle size from 46.5 (149–99 μm) to 56.38 MPa (74–49 μm). Decreasing particle size causes aggregation of the particles, which increases the compaction of the plate and results in improved strength. However further reduction in the particle



Fig. 16. SEM of the fractured surface of the composite plate without fiber content.

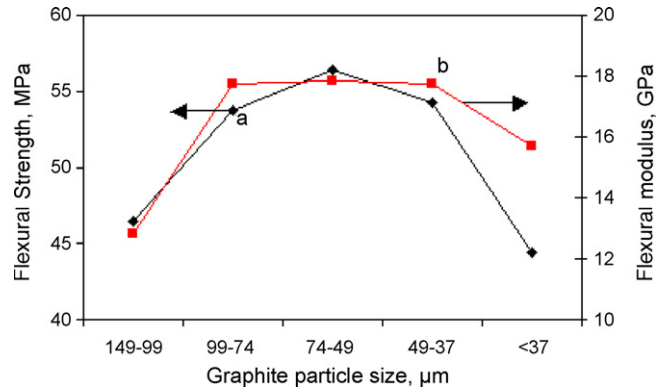


Fig. 17. Variation in the (a) flexural strength and (b) flexural modulus of the composite plate with decreasing graphite particle size.

size to less than 37 μm reduces the flexural strength of the plate. This is because reduction in the particle size will increase the number of particles. Small size graphite possesses more surface area than the longer graphite particles. Thus the graphite particles are not completely wetted by the resin. This decreased adhesion between the graphite and resin causes reduction in strength. The variation in the flexural modulus of the composite plate also shows similar behavior (Fig. 17b) as explained above.

The compressive strength of the samples with different fiber contents is shown in Fig. 18. The maximum value of the strength is achieved for 7.5 vol.% carbon fiber. The value of 84 MPa is much higher than that reported for the commercial Schunk plate (i.e. 50 MPa). The variation of the compressive strength with different particle size of graphite is plotted in Fig. 19 and shows the maximum value of 66 MPa at particle size 74–49 μm and 2.5% CF contents. Such high values are very favorable since the plate must have enough strength to maintain the dimensional integrity of the flow channels under the compressive load of the stack.

3.5. Shore hardness

The surface hardness of the composite bipolar plate increases with increasing fiber content as shown in Fig. 20. The value

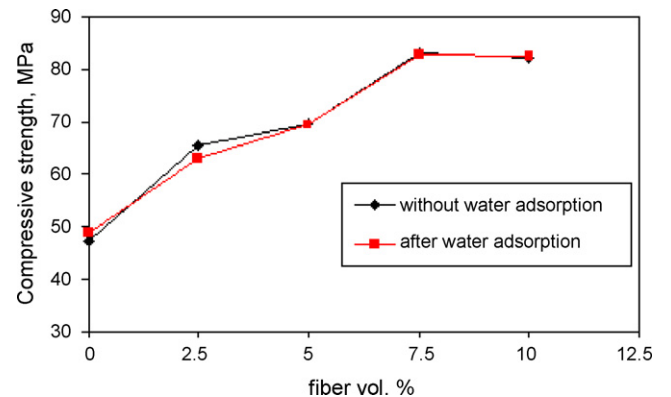


Fig. 18. Variation in the compressive strength of the composite plate with increasing fiber content.

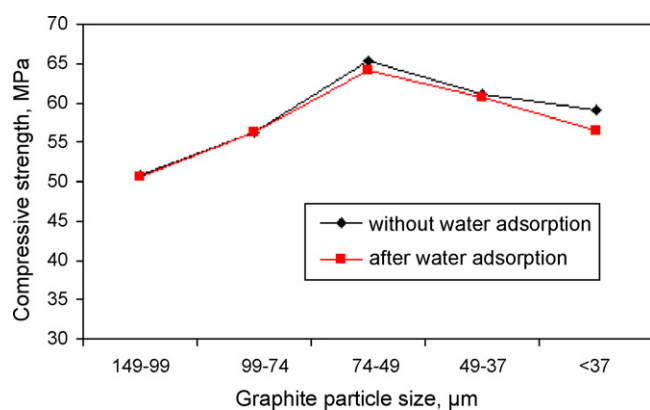


Fig. 19. Variation in the compressive strength of the composite plate with decreasing graphite particle size.

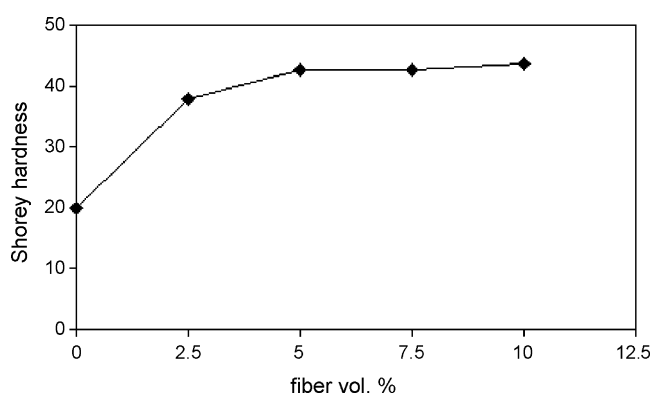


Fig. 20. Variation in the shore hardness of the composite plate with increasing fiber content.

increases from 20 to 42 as the fiber content increases from 0 to 5 vol.%. However the increase in hardness is almost negligible as the fiber content is further increased from 5 to 10 vol.%. Since the hardness value is the surface phenomena, the higher volume percent of CF in the bulk does not contribute to the hardness of the material. The shore hardness of the composite plate increases from 17 to 45 with decrease in particle size from 149–99 to <37 μm as shown in Fig. 21. Here the volume fraction of fiber is kept constant at 2.5%.

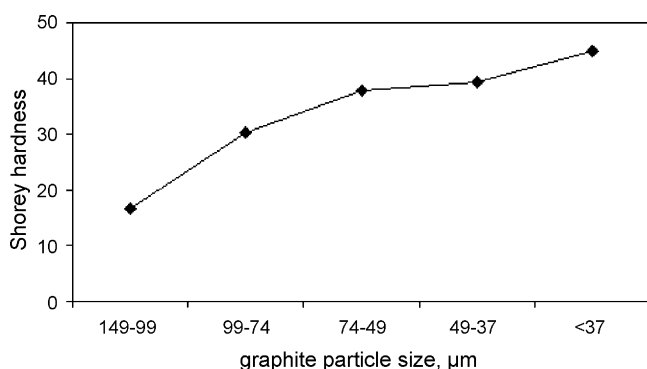


Fig. 21. Variation in the shore hardness of the composite plate with decreasing graphite particle size.

3.6. Corrosion tests

3.6.1. Corrosion resistance to acid

The most direct way to assess corrosion is to expose the material for a suitable time to an appropriate solution/pH/temperature and then measure the rate of corrosion by weight change. The bipolar plates are subjected to harsh fuel cell environment. Water withdrawn from operating PEMFC stack has been found to be acidic (pH ~1–4) at the beginning of operation, presumably as a result of leaching excess acid from the membrane. After some time the water is essentially pure at a pH of 6–7 [23].

Different bipolar plate samples were conditioned by drying the samples at 50–60 °C and their weight was noted. These were subjected to 5% H₂SO₄ solution for 5 h at 50 °C. The samples were reconditioned and were found to have the same weight as before. There was no reduction in weight that discards the possibility of any dissolution of the plate material in the acid solution.

3.6.2. Water adsorption

Since water is the by product of the fuel cell reaction which is carried out of the cell via the flow channels of the bipolar plate, it might effect the properties of the later and hence the performance of the fuel cell during prolonged operation. In our present study we have also carried out the water adsorption studies on several composite samples and the data is reported in Tables 1 and 2, respectively. The tables show that the amount of water adsorbed by almost all the samples matches the targeted value of <0.3% [18]. In order to ascertain that there is no adverse effect of water adsorption on the plates these were tested for their compressive strength before and after water adsorption. Figs. 18 and 19 show that there is no significant change in the compressive strength of the composite plate due to the small amount of water adsorbed. The values of electrical resistivity and flexural strength were also found to be similar before and after water adsorption.

3.7. Surface energy and contact angle

The bipolar plate plays a crucial role in a fuel cell and wettability is one of the most important features affecting the fuel cell performance particularly at high current densities. Since the wettability is related to the contact angle or the surface energy of the plate the above parameters were determined w.r.t. *n*-hexane and water. The values are reported in Tables 1 and 2, respectively. The data shows that the contact angle of the composite plate both with *n*-hexane and water is about 90°, which is basically due to the ordered domain structure of graphite, the major component of the composite plate. The contact angle with water suggests that the plate is partially hydrophobic and partially hydrophilic in nature. The hydrophilic tendency can result in the formation of water film on the channel walls whereas the hydrophobic nature of the plate will let the water remain in the form of droplets. While a slight pressure differential between the channel inlet and outlet may be used to reduce or eliminate the accumulation of product water, the water film can effectively reduce the hydraulic channel diameter and will increase the pressure drop

Table 1
Contact angles, surface energy and % water adsorption of the samples with different vol.% of fiber

Fiber (vol.%)	Contact angle with <i>n</i> -hexane	Contact angle with water	Surface energy (dynes cm ⁻¹)	Water absorption (%)
0	90.003	90.39	18.57	0.277
2.5	90.013	89.99	18.27	0.127
5	90.01	89.99	18.28	0.153
7.5	90.013	89.99	18.27	0.213
10	90.00	89.98	18.26	0.175

Table 2
Contact angles, surface energy and % water adsorption of the samples with different graphite particle sizes

Graphite particle size (μm)	Contact angle with <i>n</i> -hexane	Contact angle with water	Surface energy (dynes cm ⁻¹)	Water absorption (%)
149–99	90.009	89.99	18.27	0.224
99–74	90.03	89.99	18.28	0.166
74–49	90.013	89.99	18.27	0.127
49–37	89.99	90.01	18.23	0.241
<37	89.988	90.08	18.22	0.338

inside the channels. This can however lead to larger parasitic energy demands.

Film formation will also inhibit reactant gas distribution over the active area, thereby presenting a major obstacle to achieving high performance in PEM fuel cells, especially while running the cell on air for extended period of time.

As a solution to this problem, the surface of the flow field channels in one of the plates was practically made hydrophobic by PTFE (Teflon) coating on the surface of the flow fields without disturbing the current collector region. The contact angle of the teflonized part of the plate with water was found to be nearly 118° and the surface energy was reduced to 7.96 dynes cm⁻¹. The Teflon coating will eliminate even the slightest possibility of corrosion while not affecting the conductivity (since the electrons are conducted via the current collector region). The hydrophobicity introduced will not allow water to remain or form film on the surface of the flow channels and will assist in better distribution of the reactant gases.

3.8. Current–voltage performance

The bipolar plate samples with 7.5 vol.% CF, 2.5 vol.% CB and NG particle size between 74 and 49 μm, was further evaluated for single cell tests. Fig. 22 shows the comparative performance of the fuel cell with Schunk bipolar plates and NPL bipolar plates. Power density obtained from the NPL bipolar plates (572 mW cm⁻²) is nearly 83% of that obtained from the commercially available Schunk plates (690 mW cm⁻²) under identical conditions.

Fig. 22 also shows the comparative performance of the fuel cell with Schunk and NPL plates using air as an oxidant. Power density obtained from the bipolar plates developed at NPL (344 mW cm⁻²) is nearly 83% of that obtained from the commercially available standard Schunk plates (414 mW cm⁻²). Thus the power density produced in air fed regime is nearly 40% less as compared with that of oxygen operation. The problem is more pronounced in the region of higher current density. This is because of the dilution of oxidant concentration due to

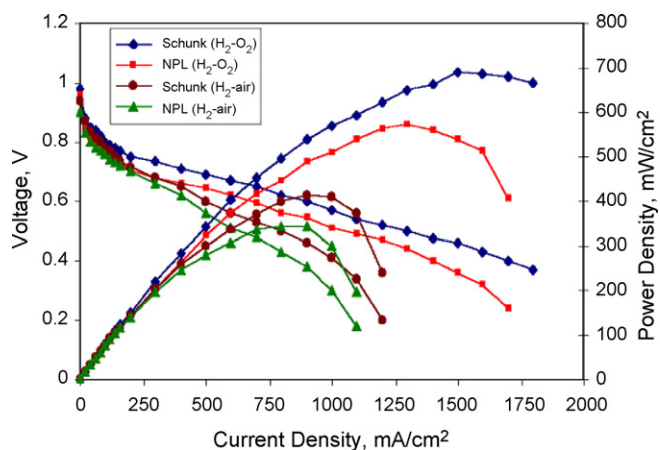


Fig. 22. Comparative performance of the fuel cell using Schunk and NPL bipolar plates.

the use of air instead of pure oxygen. The decreased partial pressure of oxygen slows down the oxygen reduction reaction and rapidly degrades cell performance. Moreover, pressuring the cathode side for circumventing this problem deteriorates the energy efficiency of the total system operation.

4. Conclusions

A carbon/polymer composite bipolar plate has been developed by making use of a carbon fiber mat (prepared by papermaking technology) as one of the filler components along with natural graphite particles and carbon black. The plate was not only conducting, impermeable and resistant to attack by moisture, acid and temperature but was also found to have excellent mechanical properties—twice than that of the commercially available plates. The plates could thus become important component in the fuel cells for the automobile sector. The high strength in the plates was achieved by sandwiching a carbon fiber skeleton preform in the carbon fillers and the polymer matrix. When tested in a PEM fuel cell, the performance with these plates achieved 83% of the power density as compared to the com-

mercially available Schunk plates. The study not only revealed the importance of carbon black as one of the reinforcements to improve the electrical conductivity but also that the size of natural graphite flakes needs to be optimum for obtaining the best performance of the composite bipolar plates.

Acknowledgements

Authors are grateful to Mr. K.N. Sood for taking the SEM pictures. Evaluation of the fuel cell performance by the scientists of Central Electrochemical Research Institute (CSIR), Chennai, is gratefully acknowledged. One of us (Priyanka H. Maheshwari) is thankful to CSIR for providing research fellowship towards the studies in the NMITLI project “Development of Fuel cells based on Hydrogen”.

References

- [1] J.M. Odgen, in: W. Vielstich, H.A. Gasteiger, A. Lamm (Eds.), *Hand Book of Fuel Cell*, vol. 3, Part 1, John Wiley & Sons, 2003, pp. 3–24, Chapter 1.
- [2] S. Lister, G. McLean, *J. Power Sources* 130 (2004) 61–76.
- [3] R.C. Makkus, A.H.H. Janssen, F.A. de Bruijn, R.A.K.M. Mallant, *Fuel Cell. Bull.* 3 (17) (2000) 5–9.
- [4] H.C. Kuan, C.C.M. Ma, Ke H. Chen, S.M. Chen, *J. Power Sources* 134 (2004) 7–17.
- [5] O.A. Velev, D.T. Tran, J.J. Kakwan, S. Gamburgzev, F. Sinoneaux, S. Srinivasan, Effect of bipolar plate materials on PEMFC performance, in: 190th Fall Meeting of the Electrochemical Society, San Antonio, TX, October 1996, abstract 101.
- [6] J. Wind, R. Spah, W. Kaiser, G. Bohm, *J. Power Sources* 105 (2002) 256–260.
- [7] D.P. Davies, P.L. Adcock, M. Turpin, S.J. Rowen, *J. Power Sources* 86 (2000) 237–242.
- [8] R. Hornung, G. Kappelt, *J. Power Sources* 72 (1998) 20–21.
- [9] R.C. Makkus, A.H.H. Janssen, F.A. de Bruijn, R.A.K.M. Mallant, *J. Power Sources* 86 (2000) 274–282.
- [10] R.J. Lawrance, Low cost bipolar current collector–separator for electrochemical cells; U.S. Patent 4,214,969 (July 1980).
- [11] E.N. Balko, R.J. Lawrance, Carbon fiber reinforced fluorocarbon-graphite bipolar current collector–separator, U.S. Patent 4,339,322 (July 1982).
- [12] T.M. Besmann, J.W. Klett, J.J. Henry Jr., E. Lara Curzio, *J. Electrochem. Soc.* 147 (2000) 4083–4091.
- [13] D.P. Wilkinson, G.J. Lamont, H.H. Voss, C. Schwab, Embossed fluid flow field plate for electrochemical fuel cells, U.S. Patent 5,521,018 (May 1996).
- [14] P.L. Hentall, J.B. Lakeman, G.O. Mepsted, P.L. Adcock, J.M. Moore, *J. Power Sources* 80 (1999) 235–241.
- [15] R.C. Emanuelson, W.L. Luoma, W.A. Taylor, U.S. Patent 4,301,222; Separator plates for electrochemical cells, Nov 17, 1981.
- [16] R.D. Breault, R.G. Martin, R.P. Roche, G.W. Scheffler, J.J. O’Brien, U.S. Patent 6,050,331; Coolant plate assembly for a fuel cell stack, April 18, 2000.
- [17] R.K. Aggarwal, D.K. Gupta, S.R. Dhakate, T.L. Dhama, R.B. Mathur, in: O.P. Bhal, V.S. Tripathi, P. Goyal (Eds.), *Indo Carbon 2006 Conference Proceedings*, Shipra Publications, Delhi, 2006, pp. 350–357.
- [18] E.A. Cho, U.S. Jeon, H.Y. Ha, S.A. Hong, I.H. Oh, *J. Power Sources* 125 (2004) 178–182.
- [19] J. Choi, T. Kim, M. Hyun, D. Peck, S. Kim, B. Lee, J. Park, D. Jung, *Carbon Sci.* 6 (3) (2005) 181–187.
- [20] R.B. Mathur, P.H. Maheshwari, T.L. Dhama, R.K. Sharma, C.P. Sharma, *J. Power Sources* 161 (2006) 790–798.
- [21] A. Aharony, D. Stauffer, in: A. Robert, Meyers (Eds.), *Encyclopedia of Physical Science and Technology*, vol. 10, Academic Press, 1987, p. 226, percolation.
- [22] <http://www.phy.mtu.edu/~jaszczak/graphprop.html>.
- [23] D.A. Shores, G.A. Deluga, in: W. Vielstich, H.A. Gasteiger, A. Lamm (Eds.), *Handbook of Fuel Cells*, vol. 3, John Wiley & Sons, 2003, pp. 273–285, Chapter 23.